Received 19 June 2018; revised 5 September 2018 and 19 September 2018; accepted 23 September 2018. Date of publication 1 October 2018; date of current version 17 December 2018. The review of this paper was arranged by Editor P. R. Berger.

Digital Object Identifier 10.1109/JEDS.2018.2872976

Gettering Sinks for Metallic Impurities Formed by Carbon-Cluster Ion Implantation in Epitaxial Silicon Wafers for CMOS Image Sensor

AYUMI ONAKA-MASADA [1,2], RYOSUKE OKUYAMA [2], SATOSHI SHIGEMATSU [2], HIDEHIKO OKUDA [2], TAKESHI KADONO [2], RYO HIROSE [2], YOSHIHIRO KOGA [2], KOJI SUEOKA [3], AND KAZUNARI KURITA [2]

1 Graduate School of System Engineering, Okayama Prefectural University, Soja 719-1197, Japan
2 Advanced Evaluation and Technology Development Department, SUMCO Corporation, Imari 849-4256, Japan
3 Department of Communication Engineering, Okayama Prefectural University, Soja 719-1197, Japan

CORRESPONDING AUTHOR: A. ONAKA-MASADA (e-mail: aonaka@sumcosi.com)

This paper is based on a paper entitled "Gettering Mechanism in Carbon-cluster-ion-implanted Epitaxial Silicon Wafers using Atom Probe Tomography" presented at the 2018 IEEE Electron Devices Technology and Manufacturing Conference.

ABSTRACT Gettering sinks for metallic impurities formed by carbon-cluster ion implantation in epitaxial silicon wafers have been investigated using technology computer-aided design and atom probe tomography (APT). We found that the defects formed by carbon-cluster ion implantation consist of carbon and interstitial silicon clusters (carbon-interstitial clusters). Vacancy-type clusters are not dominant gettering sinks for metallic impurities in the carbon-cluster ion implanted region. APT data indicated that the distribution of oxygen atoms in the defects differs between Czochralski-grown silicon and epitaxial silicon wafers. The high gettering efficiency observed in carbon-cluster ion implanted epitaxial silicon wafers in comparison with Czochralski-grown silicon wafers is due to the distribution of oxygen atoms in the defects. Defects not containing O atoms provide strong gettering sinks for metallic impurities. These defects are formed by only carbon-interstitial clusters. Oxygen atoms inside the defects modify the amount of carbon-interstitial cluster formation on the defects. It is suggested that the gettering efficiency for metallic impurities in carbon-cluster ion implanted epitaxial silicon wafer is determined by the amount of carbon-interstitial clusters.

INDEX TERMS Atom prove tomography, CMOS image sensors, gettering, ion implantation, silicon, TCAD simulation.

I. INTRODUCTION

Dark current is a key parameter of determining the performance of CMOS image sensors. For the fabrication of advanced CMOS image sensors, reduction of the dark current is an extremely important issue. Metallic impurity contamination introduced by the fabrication process is one of the causes of dark current [1]–[3]. Metallic-impurity-related defects formed in the silicon (Si) band gap allow the thermal generation of carriers. Therefore, a gettering technique is an extremely effective method for suppressing the formation of metallic-impurity-related defects during device fabrication.

It is known that void defects formed by helium (He) and hydrogen (H) implantation act as effective gettering sinks for metallic impurities [4]–[6] and reduce the dark current of CMOS image sensors [7]. The gettering occurs owing to the strain field induced by void defects, and it is called relaxation-type gettering. This gettering technique is particularly effective in samples with high concentration contamination. However, the production cost is high because the formation of void defects requires the high ($> 1 \times 10^{16}$ cm^{-2})-dose implantation of He and H ions and a long implantation time.

Our previous study on gettering using the carbon (C)-cluster ion implantation technique indicated that such implantation results in the formation of effective gettering sinks for transition-metal impurities, such as Fe, Cu, and Ni, under the active region of CMOS image sensors even in the case of low ($<1 \times 10^{15}$ cm^{-2})-dose implantation [8], [9].

2168-6734 © 2018 IEEE. Translations and content mining are permitted for academic research only.
Personal use is also permitted, but republication/redistribution requires IEEE permission.
See http://www.ieee.org/publications_standards/publications/rights/index.html for more information.

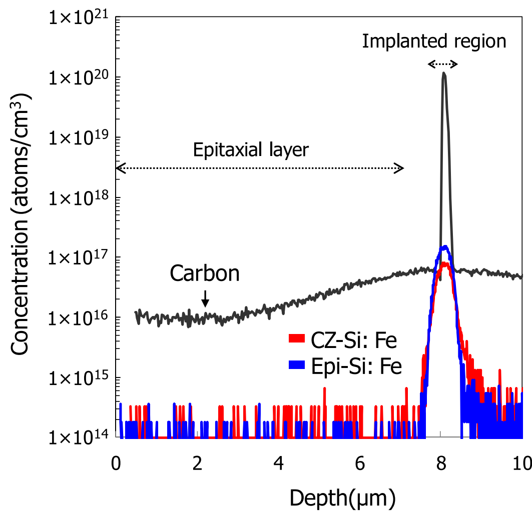

FIGURE 1. SIMS depth profiles of C and Fe concentrations in CZ-Si and Epi-Si in C-cluster ion implanted region with a dose of 1×10^{15} cm^{-2} [10].

A C-cluster ion originates from low-molecular-weight hydrocarbons (e.g., C_3H_5 and C_3H_6). It was previously suggested that C agglomerates are effective gettering sinks for metallic impurities formed by C-cluster ion implantation and that gettering occurs owing to the segregation type [9]. This gettering technique does not require impurity supersaturation, i.e., for metallic impurity gettering, sinks of the segregation type are more effective than those of the relaxation type. We have also demonstrated that the gettering efficiency of C-cluster ion implantation for Fe in the epitaxial-growth layer (Epi-Si) is approximately twice that of Czochralski (CZ)-Si (see Fig. 1), even though no secondary extended defects were observed by transmission electron microscopy (TEM) [10]. It is well known that the oxygen (O) concentration in Epi-Si is much lower than that in CZ-Si. Therefore, this result suggests that C-cluster ion implantation in a low-O-concentration layer affects C agglomerate formation or induces other point defects such as vacancy (V)-related defects. Pinacho *et al.* reported that C and interstitial Si (I) form clusters (CI clusters) in C-rich Si [11]. Okuyama *et al.* [12] have suggested that C agglomerates are formed by the aggregation of CI clusters. However, it is not clear whether O in the implanted region affects the morphology of C agglomerates. In addition, it is believed that V clusters formed by excessive V are stable configurations and can be effective gettering sinks for metallic impurities [13], [14]. It is also not clear whether V clusters are formed in a C-cluster ion implanted region. Thus, the origin of gettering sinks with high gettering efficiency in C-cluster ion implanted Epi-Si has not yet been established. Clarification of the origin of defects induced by C-cluster ion implantation in Epi-Si is very important for the fabrication of C-cluster ion implanted Si wafers with high gettering efficiency for metallic impurities.

Secondary ion mass spectrometry (SIMS) and TEM have been generally applied to the clarification of the gettering mechanism. However, in C-cluster ion implantation, the latter did not clearly demonstrate the difference in implantation defects between CZ-Si and Epi-Si owing to the limited of resolution of TEM. Additionally, these techniques are not applicable to the evaluating of the O contribution to the formation of defects, which is key issue in understand gettering sinks induced by C-cluster ion implantation in Epi-Si. Laser-assisted atom probe tomography (laser-APT) is an extremely useful approach to directly obtaining the impurity distribution at the atomic scale [15], [16]. However, there is a limit to the observable defects because APT analysis is conducted using needle-shaped samples. To overcome the problem, we have introduced implantation defects at a dose of 10^{16} cm^{-2} to increase the defect density as a model system to specify the difference in the morphology of defects between CZ-Si and Epi-Si.

In this study, we therefore investigated the morphology of defects induced by C-cluster ion implantation in detail to reveal the origin of gettering sinks for metallic impurities. First, we considered the implantation-related defect species formed by C-cluster ion implantation by performing a technology computer-aided design (TCAD) simulation. Moreover, we investigated the difference between the compositions of defects in CZ-Si and Epi-Si using APT. We also analyzed the impurity distribution of defects formed by C-cluster ion implantation.

II. THEORETICAL AND EXPERIMENTAL METHODS

We used the TCAD Sentaurus Process from Synopsys to calculate the defects formed after annealing of C-cluster ion implantation. The model of CI cluster formation is incorporated in the parameter database in the TCAD Sentaurus Process [17], whose calibration is based on the results of [11]. A cluster consisting of m substitutional C (C_s) atoms, having n atoms [either interstitial C (C_i= C_sI) or Si] existing at an interstitial position is denoted as C_mI_n. The reactions involved in C_mI_n cluster formation can be described by the following trapping and emission reactions of C_i, V, and I:

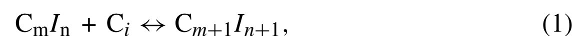

$$C_mI_n + C_i \leftrightarrow C_{m+1}I_{n+1}, \quad (1)$$

$$C_mI_n + I \leftrightarrow C_mI_{n+1}, \quad (2)$$

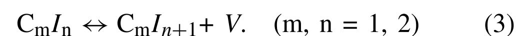

$$C_mI_n \leftrightarrow C_mI_{n+1} + V. \quad (\mathrm{m,\ n} = 1,\ 2) \quad (3)$$

Reaction 3 represents the generation of a V that diffuses away. The configurations of CI clusters taken into account in the TCAD Sentaurus Process are those up to C_3I_3. The model for V cluster formation uses the two types of V cluster model incorporated in the TCAD Sentaurus Process [17], namely, the full and 2Moment models, to reveal the formation of small V clusters and void defects. The full model is a small-V-cluster model, that is, V_n clusters with n = 2–8 are included. The V_n clusters included in this model act as precursors of void defects. V_n cluster formation can be described by the following reactions:

$$V_n + V \leftrightarrow V_{n+1}, \quad (4)$$

$$V_n + I \leftrightarrow V_{n-1}. \quad (n = 1, 2 \ldots) \tag{5}$$

The 2Moment model calculates the formation and dissolution of V_2, and a V_n cluster with n>2 is defined as a void defect. Both models for V cluster formation are incorporated in the parameter database, whose calibration is based on the results in [18] and [19]. In this calculation, we used the C-cluster ion of C_3H_6, a dose of 1×10^{16} cm^{-2}, an implantation energy of 80 keV, and heat treatment at 1100 °C for 30 min.

The samples subjected to C-cluster ion implantation were n-type phosphorus-doped CZ-Si and Epi-Si wafers. The interstitial O concentration in the CZ-Si was about 1.4×10^{18} cm^{-3} and that of the C-cluster ion-implanted region in Epi-Si was below 10^{16} cm^{-3}. C-cluster ions of C_3H_6 were implanted into wafers with an energy of 80 keV at a dose of 1×10^{16} cm^{-2}. After implantation, the samples were annealed at 1100 °C for 30 min in N_2 ambient. The C depth profiles were measured by SIMS. For APT analysis, needle-shaped samples including the C-cluster ion implanted region were fabricated using a focused ion beam (FIB) system. A Ni capping layer was deposited on the sample surface for protection against FIB damage. Figure 2 shows the experimental procedure of this study. The APT analysis was carried out using a laser-assisted APT system (AMETEK LEAP 4000XSi) equipped with an ultraviolet laser (wavelength of 355 nm, laser power of 20 pJ) to examine the impurity distribution in the C-cluster ion implanted region. The samples were cooled to 70 K. The APT data were analyzed using integrated visualization and analysis software (IVAS) from CAMECA.

III. RESULTS AND DISCUSSION

A. DEFECT SPECIES FORMED BY C-CLUSTER ION-IMPLANTATION SIMULATED BY TCAD

Figure 3 shows the C, V, and I depth profiles resulting from the implantation of 1×10^{16} cm^{-2} C_3H_6 ions into the Si wafer at 80 keV obtained by simulation. The calculated depth profiles of V and I are nearly the same. These calculation results do not agree with those of Si ion implantation, which showed impurity gettering via V clusters [14], which is probably due to the low energy implantation of C-cluster ions. Figure 4 shows C depth profiles obtained from the TCAD simulation and SIMS analysis of the implantation of 1×10^{16} cm^{-2} C_3H_6 ions into CZ-Si and Epi-Si after annealing at 1100 °C for 30 min. The total V concentration calculated by using the two types of cluster model after annealing is also shown in Fig. 4. Note that in the TCAD simulation, the O concentration in the Si substrate cannot be taken into account. The C depth profiles of both CZ-Si (red dotted line) and Epi-Si (blue line) obtained from SIMS are in good agreement as shown in Fig. 4. In addition, although the agreement is not perfect, total C profile obtained by TCAD simulation was similar to the SIMS C depth profiles. The TCAD simulation results indicate that the C profile in the C-cluster ion implanted region is formed by CI clusters. The C profile is mainly formed by C_3I_3 clusters. This result is in good agreement with a previous study on C_3H_5 ions with a lower dose implantation of 5×10^{14} cm^{-2} [20].

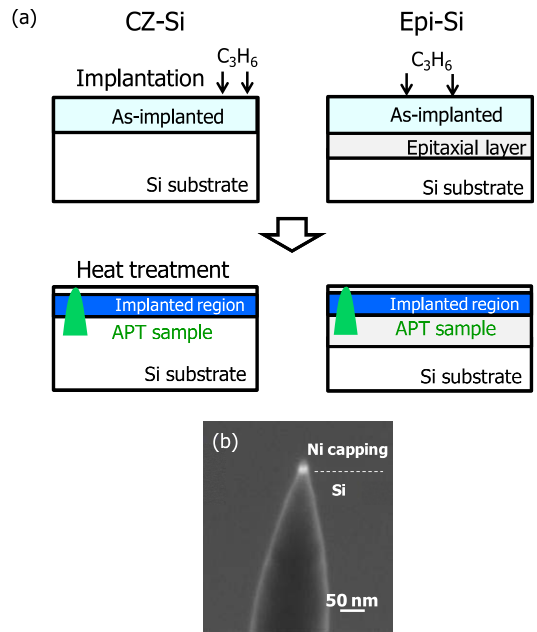

FIGURE 2. (a) Schematic illustration of experimental procedure of this study. (b) Needle shaped sample for APT analysis.

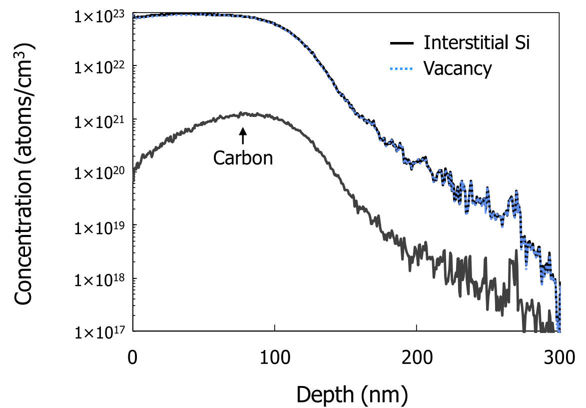

FIGURE 3. The depth profiles of C, I, and V after C-cluster ion implantation at dose of 1×10^{16} cm^{-2} calculated by TCAD simulation.

On the other hand, hardly any V clusters including void defects form in the C-cluster ion-implanted region, although V_6 clusters have been reported to have particularly stable configurations [19], [21]. Positron annihilation spectrometry studies have indicated that V defects decrease in number or disappear during heat treatment above 850 °C [22]. This supports the low V cluster concentration after 1100 °C heat treatment observed in the TCAD simulation. It is probable that during heat treatment at the high temperature of 1100 °C, the out diffusion of V is the dominant reaction rather than V cluster formation. The contribution of V to CI cluster formation represented by reaction 3 also suppressed the formation of V cluster. In addition, the TCAD simulation results did not indicate an increase in the V cluster concentration in

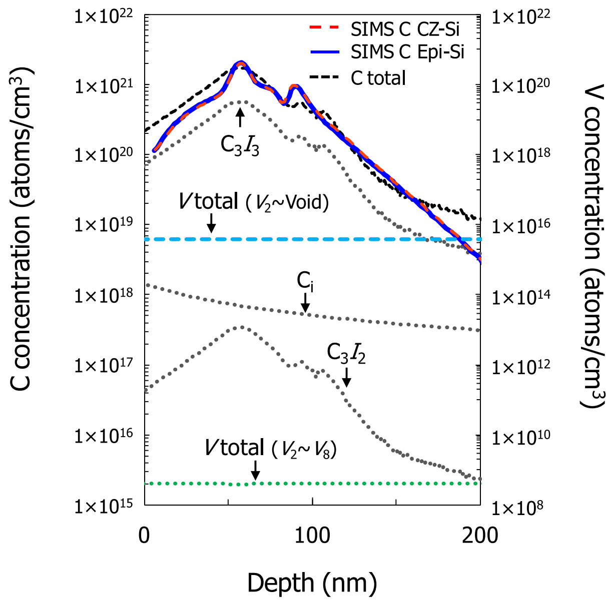

FIGURE 4. The depth profiles of C and V clusters after at 1100 °C for 30 min heat treatment with a C_3H_6 dose of 1 × 10^{16} cm^{-2} by TCAD simulation. The black dotted line represent carbon total obtained by TCAD simulation, the red dotted line and blue line are by SIMS measurement.

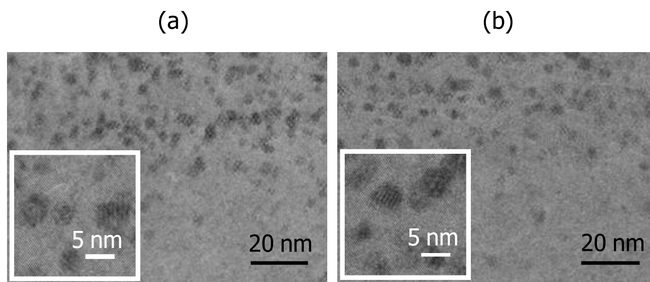

FIGURE 5. Cross-sectional TEM images of (a) CZ-Si and (b) Epi-Si implanted at a C-cluster ion implantation dose of 1 × 10^{16} cm^{-2} after annealing at 1100 °C for 30 min.

the C-cluster ion-implanted region in both V cluster models. If metallic impurity gettering occurs through V clusters, an increase in the V cluster concentration should be observed because the high gettering efficiency for metallic impurities mirrors the C profile in the C-cluster ion implanted region, as shown in Fig. 1 [10]. The gettering reaction through V clusters should be promoted by the increased solubility of the metallic impurities in region where the V cluster formed [13], [14]. Additionally, in the case of relaxation gettering via void defects, 20–35 nm diameter octahedral size defects should form in the ion implanted region [4]–[7]. However, in cross-sectional TEM images of C-cluster ion implanted CZ-Si and Epi-Si, no void defects were observed in the ion implanted region, as shown in Fig. 5. Only the 5 nm size defects were observed in both samples, which are probably C agglomerates. Thus, we consider that V clusters are not dominant gettering sinks for metallic impurities in the C-cluster ion implanted region in both CZ-Si and Epi-Si.

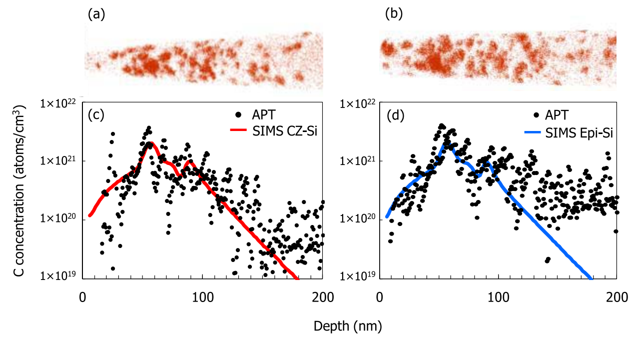

FIGURE 6. The three-dimensional APT maps of C in C-cluster ion implanted (a) CZ-Si and (b) Epi-Si after heat treatment. The one-dimensional C concentration profiles in CZ-Si and Epi-Si are shown in (c) and (d), respectively. The black circles represent the result obtained by APT and red and blue lines represent the result in CZ-Si and Epi-Si obtained by SIMS, respectively.

These simulation results suggest that the gettering of metallic impurities occurs by the interaction with CI clusters such as C_3I_3 in both CZ-Si and Epi-Si. Thus, we consider that the amount of metallic impurity gettering depends on the amount of CI cluster formation in the C-cluster ion-implanted region. We assume that the O concentration in the C-cluster ion implanted region may affect the amount of CI cluster formation.

B. THREE-DIMENSIONAL MORPHOLOGY OF DEFECTS INDUCED BY C-CLUSTER ION-IMPLANTED CZ-SI AND EPI-SI

Figures 6(a) and 6(b) show three-dimensional C-atom maps in the C-cluster ion implanted region in CZ-Si and Epi-Si, respectively. It has been reported that the C concentration increases at the center of C agglomerates in both samples [23]. It can be seen that the C agglomerates formed by C-cluster ion implantation in Epi-Si are similar to those in CZ-Si. Additionally, in both samples, it is considered that the C agglomerates observed by APT correspond to the defects observed by TEM shown in Fig. 5 [9]. Figures 6(c) and 6(d) show the one-dimensional C concentration profiles obtained from the APT data in the depth direction together with the SIMS profiles. Although the APT profiles have a discrete distribution, it can be seen that they are in good agreement with the SIMS profiles. The TCAD simulation results shown in Fig. 4 indicate that the C profiles in the C-cluster ion implanted region consist of CI clusters formed by the interaction with C and I. Thus, we consider that the C agglomerates observed by APT analysis are agglomerates of CI clusters such as C_3I_3 in both CZ-Si and Epi-Si.

What is the role of O in the C-cluster ion implanted region in C agglomerate formation? To investigate the role of O, we analyzed the difference between the distributions of O and C atoms in both CZ-Si and Epi-Si obtained from the APT mapping. Figures 7(a) and 7(b) show isoconcentration surfaces defined at 5 at.% C and 1.2 at.% O in both CZ-Si and Epi-Si,

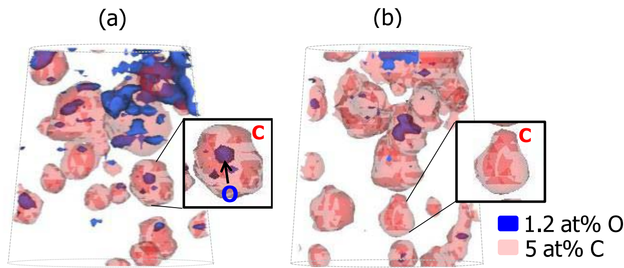

FIGURE 7. The isoconcentration surfaces associated with 1.2 at% O and 5 at% C in C-cluster ion implanted (a) CZ-Si and (b) Epi-Si. The C agglomerate containing and not containing O atoms are shown in (a) and (b), respectively.

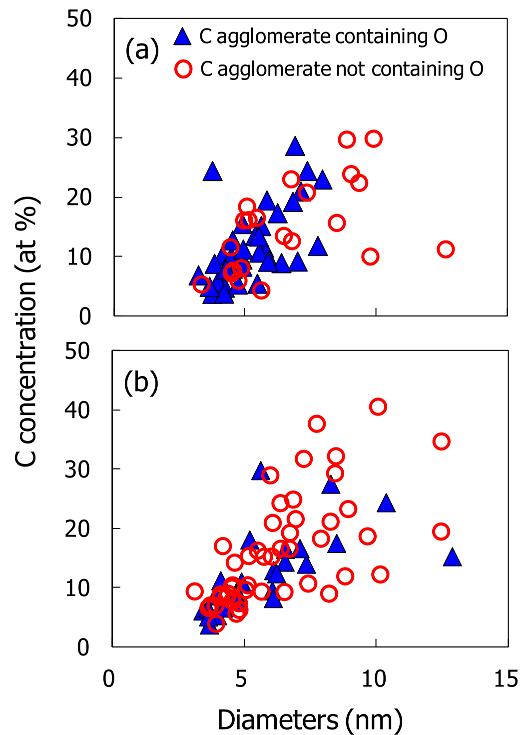

FIGURE 8. Relationship between diameters of C agglomerates and C concentration for (a) CZ-Si and (b) Epi-Si. The blue triangle represent the C agglomerates containing O atoms and the red circles represent the C agglomerates not containing O atoms [23].

respectively, to more clearly illustrate the distribution of O in C agglomerates. The figures show APT data obtained at depths of 40–90 nm, which include the region of maximum C concentration observed by SIMS shown in Fig. 6. The 5 at.% C and 1.2 at.% O isoconcentration-surface means delineate the regions containing more than 5 at.% C and 1.2 at.% O, respectively. Figure 7(a) indicates the presence of O atoms incorporated inside C agglomerates. The data suggest that these agglomerates grew by incorporating O atoms. On the other hand, the C agglomerates shown in Fig. 7(b) consist of only C atoms and were probably formed by the aggregation of C*I* clusters. By focusing on C and O distribution, it was found that the C agglomerates can be divided into two types; those including and not including O atoms.

Figure 8 shows the relationship between the diameter of the C agglomerates and the maximum C concentration at the agglomerate centers. The results for the two types of C agglomerates are also shown in Fig. 8. The average size of the C agglomerates estimated using IVAS was approximately 5 nm in both samples. However, it appears that the C concentration of the agglomerate formed by the implantation of Epi-Si had a higher central C concentration than that formed by the implantation of CZ-Si. Moreover, comparing CZ-Si and Epi-Si, the ratio of the number of the two types of defects differs. The results indicated that more C agglomerates in CZ-Si contained O atoms. On the other hand, in Epi-Si, there were more C agglomerates that did not contain O atoms. The proportion of C agglomerates not containing O atoms in Epi-Si was approximately two times that in CZ-Si. This suggests that the atomic-level defect compositions induced by C-cluster ion-implantation in CZ-Si and Epi-Si differ, despite the apparent similarity of the agglomerates.

It is believed that the formation of C agglomerates cannot occur without the relaxation of stress due to the incorporation of *I* or O because agglomerate formation by C itself leads to a decrease in volume [24]. If the C agglomerates are formed by relaxation of stress, the amount of C*I* cluster formation will depend on the amount of O incorporated in the agglomerates. Therefore, it is considered that the amount of C*I* clusters formation in the C agglomerates differs between those containing O atoms and those not containing O atoms. The APT data illustrated in Fig. 8 show that C-cluster ion implanted Epi-Si has more C agglomerates not containing O atoms than those containing O atoms. This suggests that Epi-Si has more C agglomerates only consisting of C*I* clusters. In other words, in Epi-Si, the most of implanted C contributes to C*I* cluster formation such as C_3I_3. On the other hand, in CZ-Si, because a large amount of O is contained in the C-cluster ion-implanted region, the formation of C agglomerates involves not only *I* but also O atoms. The presence of C agglomerates containing O atoms suggests that part of the implanted C contributes to the interaction with O such as CO defect formation.

Recent theoretical results by first-principles calculation suggest that C*I* clusters such as C_3I_3 can be effective gettering sinks for metallic impurities [25]. On the other hand, C trapped by O atoms cannot be effective gettering sinks [26]. These calculation results indicate that C agglomerates formed by C*I* clusters undergo a strong electronic interaction with metallic impurities. Hence, the amount of C*I* cluster formation in the C-cluster ion implanted region determines the gettering efficiency for metallic impurities. The O atoms in C agglomerates probably suppress the electronic interaction of agglomerates because they inhibit C*I* cluster formation. We propose that the increase in the solid solubility of metallic impurities in C-cluster ion implanted Epi-Si is due to the strong electronic interaction of C agglomerates consisting of C*I* clusters. The mechanisms are illustrated in Fig. 9.

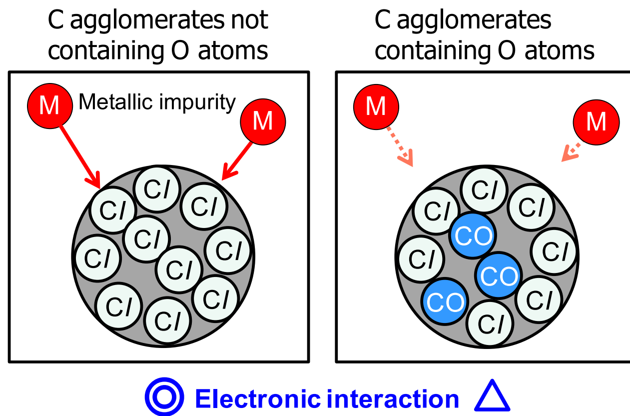

FIGURE 9. **Illustration of model of gettering reaction for metallic impurity on C agglomerates formed by C-cluster ion implantation.**

IV. CONCLUSION

We investigated the origin of gettering sinks for metallic impurities induced by C-cluster ion implantation in Epi-Si using TCAD simulation and APT. The TCAD simulation results indicated that not point defect clusters but C*I* clusters in the C-cluster ion implanted region provide gettering sinks for metallic impurities. We found by APT that the C agglomerates are aggregations of C*I* clusters in both CZ-Si and Epi-Si. The APT results indicated that the distribution of O atoms in C agglomerates differs between CZ-Si and Epi-Si. The C-cluster ion implanted Epi-Si induced more defects not containing O atoms than those containing O atoms inside C agglomerates. This indicates that more C agglomerates only consist of C*I* clusters. The O atoms inside C agglomerates inhibit C*I* cluster formation. We consider that the gettering efficiency for metallic impurities in the C-cluster ion implanted region is determined by the amount of C*I* cluster formation. The obtained results indicate that the control of O atoms inside the defects induced by C-cluster ion implantation is effective for maximizing the localization for metallic impurities to reduce the dark current.

REFERENCES

[1] W. C. Mccolgin, J. P. lavine, and C. V. Stancampiano, "Dark current spectroscopy of metals in silicon," in *Proc. MRS Fall Meeting*, Boston, MA, USA, 1997, pp. 187–192.

[2] F. Domengie, J. L. Regolini, and D. Bauza, "Study of metal contamination in CMOS image sensors by dark-current and deep-level transient spectroscopies," *J. Electron. Mater.*, vol. 39, no. 6, pp. 625–629, Jan. 2010, doi: 10.1007/s11664-010-1212-6.

[3] J.-P. Carrère, S. Place, J.-P. Oddou, D. Beuoit, and F. Roy, "CMOS image sensor: Process impact on dark current," in *Proc. IRPS*, Waikoloa, HI, USA, 2014, pp. 3C.1.1–3C.1.6.

[4] B. Mohadjeri, J. S. Williams, and J. Wong-Leung, "Gettering of nickel to cavities in silicon introduced by hydrogen implantation," *Appl. Phys. Lett.*, vol. 66, no. 15, pp. 1889–1891, Apr. 1995, doi: 10.1063/1.113311.

[5] J. Wong-Leung, C. E. Ascheron, M. Petravic, R. G. Elliman, and J. S. Williams, "Gettering of copper to hydrogen-induced cavities in silicon," *Appl. Phys. Lett.*, vol. 66, no. 10, pp. 1231–1233, Mar. 1995.

[6] S. M. Myers and D. M. Follstaedt, "Interaction of copper with cavities in silicon," *J. Appl. Phys.*, vol. 79, no. 3, pp. 1337–1350, Feb. 1996, doi: 10.1063/1.361031.

[7] I.-H. Kim, J.-S. Park, T.-H. Shim, and J.-G. Park "Si CMOS image-sensors designed with hydrogen-ion implantation induced nanocavities for enhancing output voltage sensing margin via proximity gettering," *IEEE Trans. Electron Devices*, vol. 64, no. 5, pp. 2345–2349, May 2017, doi: 10.1109/TED.2017.2677948.

[8] K. Kurita *et al.*, "Proximity gettering of C_3H_5 carbon cluster ion-implanted silicon wafers for CMOS image sensors: Gettering effects of transition metal, oxygen, and hydrogen impurities," *Jpn. J. Appl. Phys.*, vol. 55, no. 12, Dec. 2016, Art. no. 121301, doi: 10.7567/JJAP.55.121301.

[9] K. Kurita *et al.*, "Proximity gettering technology for advanced CMOS image sensors using carbon cluster ion-implantation technique: A review," *Phys. Status Solidi A*, vol. 214, no. 7, Jul. 2017, Art. no. 1700216, doi: 10.1002/pssa.201700216.

[10] A. Onaka-Masada *et al.*, "Effect of low-oxygen-concentration layer on iron gettering capability of carbon-cluster ion-implanted Si wafer for CMOS image sensors," *Jpn. J. Appl. Phys.*, vol. 57, no. 2, Feb. 2018, Art. no. 021304, doi: 10.7567/JJAP.57.021304.

[11] R. Pinacho *et al.*, "Carbon in silicon: Modeling of diffusion and clustering mechanisms," *J. Appl. Phys*, vol. 92, no. 3, pp. 1582–1587, Aug. 2002, doi: 10.1063/1.1489715.

[12] R. Okuyama *et al.*, "Effect of dose and size on defect engineering in carbon cluster implanted silicon wafers," *Jpn. J. Appl. Phys.*, vol. 57, no. 1, Jan. 2018, Art. no. 011301, doi: 10.7567/JJAP.57.011301.

[13] R. Krause-Rehberg *et al.*, "Identification of getter defects in high-energy self-implanted silicon at $R_p/2$," *Physica B Condensed Matter*, vols. 308–310, pp. 442–445, Dec. 2001, doi: 10.1016/S0921-4526(01)00717-7.

[14] R. A. Brown *et al.*, "Impurity gettering to secondary defects created by MeV ion implantation in silicon," *J. Appl. Phys.*, vol. 84, no. 5, pp. 2459–2465, May 1998, doi: 10.1063/1.368438.

[15] K. Thompson, P. L. Flaitz, P. Ronsheim, D. J. Larson, T. F. Kelly, "Imaging of arsenic Cottrell atmospheres around silicon defects by three-dimensional atom probe tomography," *Science*, vol. 317, no. 7, pp. 1370–1374, Sep. 2007, doi: 10.1126/science.1145428.

[16] K. Hoummada, D. Mangelinck, B. Gault, and M. Cabié, "Nickel segregation on dislocation loops in implanted silicon," *Scripta Materialia*, vol. 64, no. 5, pp. 378–381, Mar. 2011, doi: 10.1016/j.scriptamat.2010.10.036.

[17] *Synopsys Sentaurus Process User's Manual, Release, 9*, Synopsys Inc., Zürich, Switzerland, 2014.

[18] M. Prasad and T. Sinno, "Internally consistent approach for modeling solid-state aggregation. I. Atomistic calculations of vacancy clustering in silicon," *Phys. Rev. B, Condens. Matter*, vol. 68, no. 4, Jul. 2003, Art. no. 045206, doi: 10.1103/PhysRevB.68.045206.

[19] "Advanced front-end technology modeling for ultimate integrated circuits," IST Project, Islamabad, Pakistan, Rep. 027152, Oct. 2009.

[20] R. Okuyama *et al.*, "Trapping and diffusion behaviour of hydrogen simulated with TCAD in projection range of carbon-cluster implanted silicon epitaxial wafers for CMOS image sensors," *Phys. Status Solidi C*, vol. 14, no. 7, Jul. 2017, Art. no. 1700036, doi: 10.1002/pssc.201700036.

[21] J. L. Hastings, S. K. Estreicher, and P. A. Fedders, "Vacancy aggregates in silicon," *Phys. Rev. B, Condens. Matter*, vol. 56, no. 16, pp. 10215–10220, Oct. 1997, doi: 10.1103/PhysRevB.56.10215.

[22] R. Krause-Rehberg and H. S. Leipner, "Determination of absolute vacancy concentrations in semiconductors by means of positron annihilation," *Appl. Phys. A, Solids Surf.*, vol. 64, no. 5, pp. 457–466, May 1997.

[23] A. Onaka-Masada *et al.*, "Gettering mechanism in carbon-cluster-ion-implanted epitaxial silicon wafers using atom probe tomography," in *Proc. EDTM*, Kobe, Japan, 2018, pp. 166–168.

[24] W. J. Taylor, T. Y. Tan, and U. Gösele, "Carbon precipitation in silicon: Why is it so difficult?" *Appl. Phys. Lett.*, vol. 62. no. 25, pp. 3336–3338, Apr. 1993, doi: 10.1063/1.109063.

[25] Y. Jin and S. T. Dunham, "Modeling of carbon clustering and associated metal gettering," *ECS Trans.*, vol. 64. no. 11, pp. 211–218, 2014, doi: 10.1149/06411.0211ecst.

[26] S. Shirasawa, K. Sueoka, T. Yamaguchi, and K. Maekawa, "Density functional theory calculations for estimation of gettering sites of C, H, intrinsic point defects and related complexes in Si wafers," *Mater. Sci. Semicond. Process.*, vol. 44, pp. 13–17, Mar. 2016, doi: 10.1016/j.mssp.2016.01.001.

AYUMI ONAKA-MASADA was born in Himeji, Japan, in 1985. She received the B.E. degree in applied chemistry from the University of Hyogo, Kobe, Japan, in 2008 and the M.S. degree in chemistry from Osaka University, Osaka, Japan, in 2010. She is currently pursuing the Ph.D. degree with Okayama Prefectural University, Okayama, Japan. In 2010, she joined SUMCO Corporation, Japan. She worked in research and development group in the area of metallic impurity contamination analysis in silicon wafer using deep level transient spectroscopy. She is currently research in gettering technology for advanced CMOS image sensor.

RYOSUKE OKUYAMA was born in Sasebo, Japan, in 1983. He received the B.E. degree in materials science and engineering and the M.E. degree in materials physics and chemistry from Kyushu University, Fukuoka, Japan, in 2006 and 2008, respectively. From 2009 to 2012, he was a Researcher with Nano-SOI Process Laboratory, Hanyang University, South Korea. His main research interests include kinetic analysis of hydrogen diffusion behavior and passivation effect in hydrocarbon molecule ion implanted wafers for advanced CMOS image sensors.

SATOSHI SHIGEMATSU was born in Chikushino, Japan, in 1990. He received the B.Sc. and M.Sc. degrees in physics from Kagoshima University, Kagoshima, Japan, in 2014 and 2016, respectively. Since 2016, he has been researching a gettering behavior of molecular ion implanted silicon wafers in atomic scale using atom probe tomography in SUMCO Corporation, Tokyo, Japan.

HIDEHIKO OKUDA was born in Isahaya, Japan, in 1966. He received the B.E. degree in materials engineering from Nagasaki University, Nagasaki, Japan, in 1993. In 1993, he joined SUMCO Corporation. His current work is development of annealing process for high quality Si wafer.

TAKESHI KADONO was born in Sasebo, Japan, in 1984. He received the B.E. degree in materials physics and engineering and the M.E. degree in applied physics from Miyazaki University, Japan, in 2007 and 2009, respectively. In 2009, he joined SUMCO Corporation, Tokyo, Japan. His current work is product design development of hydrocarbon molecular ion implanted silicon wafers.

RYO HIROSE was born in Kyoto, Japan. He received the B.E. degree in chemical science and engineering and the M.S. degree in chemistry from Osaka University, Japan, in 2012 and 2014, respectively, where he is currently pursuing the Ph.D. degree with the Department of Nuclear Engineering, Kyoto University. In 2014, he joined SUMCO Corporation, Tokyo, Japan. He working on the development of new gettering technique for advanced CMOS image senor using multielement molecular ion implantation.

YOSHIHIRO KOGA was born in Fukuoka, Japan, in 1971. He received the B.E. and M.E. degrees from the Department of Electrical and Electronic Engineering, Nagoya Institute of Technology in 1995 and 1998, respectively. From 1998 to 2006, he developed power devices with Oki Electric Industry Company, Ltd. He has been developed semiconductor materials for CMOS image sensor and power devices with SUMCO Corporation.

KOJI SUEOKA was born in Shizuoka, Japan, in 1963. He received the B.E., M.E., and Ph.D. degrees from Kyoto University, Kyoto, Japan, in 1987, 1989, and 1997, respectively. He joined Sumitomo Metal Industries, Hyogo, Japan, in 1989. Since 2003, he has been with the Department of Communication Engineering, Okayama Prefectural University, where he is currently a Professor. His main areas of research interests are defect engineering in silicon, especially intrinsic point defects and impurity gettering.

KAZUNARI KURITA was born in Hamamatsu, Japan. He received the B.E. degree in electronics engineering from Akita University, Akita, Japan, in 1991, the M.E. degree in electronics engineering from Tohoku University, Sendai, Japan, in 1993, and the Ph.D. degree in electrical and electronics engineering from the Kanagawa Institute of Technology, Atsugi, Japan, in 2002. From 1993 to 2001, he was a Research Member with the Central Research Institute of Mitsubishi Materials Corporation, Omiya Saitama, Japan. In 2002, he joined SUMCO Corporation, Tokyo, Japan. He invented the novel gettering technology for advanced CMOS image senor using hydrocarbon molecular ion implantation technique. He has published 30 peer reviewed papers covering gettering technology for CMOS image sensor and is the holder of over 100 Japan and U.S. patents. His current research interests include the silicon wafer gettering process and the development of metallic impurity contamination analysis techniques, such as deep level transient spectroscopy and microwave photo-conductance decay lifetime measurement techniques. Since 2016, he has been a General Manager of Research and Development Division, SUMCO Corporation. He was a recipient of the Honorary Award the 23rd SSSJ Technical Award from the Surface Science Society of Japan in 2017.